Beta-caryophyllene protects against alcoholic steatohepatitis by attenuating inflammation and metabolic dysregulation in mice

Running Title: Beta-caryophyllene is hepatoprotective

Zoltan V. Varga[1], Csaba Matyas[1], Katalin Erdelyi[1], Resat Cinar[2], Daniela Nieri[3], Andrea Chicca[3], Balazs Tamas Nemeth[1], Janos Paloczi[1], Tamas Lajtos[1], Lukas Corey[1], Gyorgy Hasko[4], Bin Gao[5], George Kunos[2], Jürg Gertsch[3] and Pal Pacher[1]

Affiliations:

[1]Laboratory of Cardiovascular Physiology and Tissue Injury, National Institutes of Health/NIAAA, Bethesda, MD 20852, USA.

[2]Laboratory of Physiologic Studies, National Institutes of Health/NIAAA, Bethesda, MD 20852, USA.

[3]Institute of Biochemistry and Molecular Medicine, National Center of Competence in Research TransCure, University of Bern, CH-3012 Bern, Switzerland.

[4]Departments of Surgery, Rutgers New Jersey Medical School, Newark, NJ 07103, USA.

[5]Laboratory of Liver Diseases, National Institutes of Health/NIAAA, Bethesda, MD 20852, USA.

Contact:

Pal Pacher, MD, PhD, FAHA, FACC

Laboratory of Cardiovascular Physiology and Tissue Injury

5625 Fishers Lane, Room 2N-17; Bethesda, MD 20892-9413

Phone: (301)443-4830 Email: pacher@mail.nih.gov

Conflict of interest disclosure: All Authors declare no conflict of interest.

This article has been accepted for publication and undergone full peer review but has not been through the copyediting, typesetting, pagination and proofreading process which may lead to differences between this version and the Version of Record. Please cite this article as doi: 10.1111/bph.13722

This article is protected by copyright. All rights reserved.

Tables of links

TARGETS
GPCRs[b]
cannabinoid 1 receptor
cannabinoid 2 receptor
Nuclear hormone receptors[c]
peroxisome proliferator-activated receptor-α
Enzymes[e]
3-hydroxy-3-methylglutaryl-CoA synthase 2
arginase I
cyclooxygenase 2
fatty acid amide hydrolase
sirtuin-1
LIGANDS
2-arachidonoylglycerol
anandamide
arachidonic acid
chemokine (C-C motif) ligand 2
chemokine (C-C motif) ligand 4
chemokine (C-X-C motif) ligand 2
intercellular adhesion molecule 1
interleukin 1 beta
interleukin 10
interleukin-6
N-oleoylethanolamide
tumor necrosis factor alpha

Accepted Article

This article is protected by copyright. All rights reserved.

Abbreviations

4-HNE: 4-hydroxynonenal

ALT: alanine aminotransferase

ARG1: arginase 1

BCP: beta-caryophyllene

CB1: cannabinoid receptor type 1

CB2: cannabinoid receptor type 2

CCL2: monocyte chemoattractant protein - MCP1

CCL4: Chemokine (C-C motif) ligand 4 - Macrophage inflammatory protein-1β - MIP-1β

CD11b: cluster of differentiation molecule 11B

CD32: cluster of differentiation 32

CD34: cluster of differentiation 34

CD117: cluster of differentiation 117

CD163: cluster of differentiation 163

CD68: cluster of differentiation 68

CLEC7A: C-type lectin domain family 7 member A

COX-2: cyclooxygenase-2 or prostaglandin-endoperoxide synthase 2

CXCL2: macrophage inflammatory protein 2-alpha - MIP2-alpha

DMSO: dimethyl sulfoxide

ECL: enhanced chemiluminescence

This article is protected by copyright. All rights reserved.

EDTA: ethylenediaminetetraacetic acid

F4/80: EGF-like module-containing mucin-like hormone receptor-like 1

FAAH: fatty acid amide hydrolase

FDA: Food and Drug Administration

FFPE: formalin-fixed, paraffin-embedded tissue samples

FGF21: fibroblast growth factor 21

FOXO1: forkhead box protein O1

FOXO3: forkhead box O3

G6PC: glucose-6-phosphatase

GC/MS: gas chromatography / mass spectrometry

H_2O_2: hydrogen peroxide

HMGB1: high-mobility group protein 1

HMGCS2: 3-hydroxy-3-methylglutaryl-CoA synthase 2

IBA-1: ionized calcium-binding adapter molecule 1

ICAM-1: intercellular adhesion molecule 1

IL10: interleukin 10

IL1ß: interleukin 1 beta

IL-6: interleukin 6

LY6G: lymphocyte antigen 6 complex locus G6D

MGL1/CD301: macrophage galactose-type C-type lectin 1

This article is protected by copyright. All rights reserved.

MRC2: mannose receptor C type 2

NAD^+: nicotinamide adenine dinucleotide

NIAAA: National Institute on Alcohol Abuse and Alcoholism

PBS: phosphate-buffered saline

PCK1: phosphoenolpyruvate carboxykinase 1

PFK: phosphofructokinase

PGC1α : peroxisome proliferator-activated receptor gamma coactivator 1- alpha

PGC-1ß: peroxisome proliferator-activated receptor gamma coactivator 1- beta

PPAR-α : peroxisome proliferator-activated receptor alpha

RIPA: radioimmunoprecipitation assay buffer

SIRT-1: NAD-dependent deacetylase sirtuin-1

SREBP1c: sterol regulatory element-binding protein 1

TBS-T: Tris-buffered saline with Tween 20

Accep

This article is protected by copyright. All rights reserved.

Abstract

Background and aims: Beta-caryophyllene (BCP) is a plant-derived FDA approved food additive with anti-inflammatory properties. Some of its beneficial effects *in vivo* reported to involve activation of cannabinoid 2 receptors (CB2) that are predominantly expressed in immune cells. Herein, we evaluated the translational potential of BCP using a well-established model of chronic and binge alcohol-induced liver injury.

Methods: In this study we investigated the effects of BCP on liver injury induced by chronic plus binge alcohol feeding in mice *in vivo* by using biochemical assays, real-time PCR and histology analyses. Serum and hepatic BCP levels were also determined by GC/MS.

Results: Chronic treatment with BCP attenuated the chronic and binge alcohol-induced liver injury and inflammation by attenuating the pro-inflammatory phenotypic `M1` switch of Kupffer cells and by decreasing the expression of vascular adhesion molecules ICAM-1, E-Selectin and P-Selectin, as well as the neutrophil infiltration. It also beneficially influenced hepatic metabolic dysregulation (steatosis, protein hyperacetylation, and PPAR-α signaling). The above mentioned protective effects of BCP against alcohol-induced liver injury were attenuated in CB2 knockout mice, indicating that the beneficial effects of this natural product in liver injury involve CB2 receptor activation. Following acute or chronic administration BCP was detectable both in the serum and liver tissue homogenates but not in the brain.

Conclusions: Given the safety of BCP in humans this food additive has a high translational potential in treating or preventing hepatic injury associated with oxidative stress, inflammation and steatosis.

Accepted Article

This article is protected by copyright. All rights reserved.

Introduction

Beta-caryophyllene (BCP) is a bicyclic sesquiterpene found in larger amounts in numerous essential oils of food plants from cloves, basil, and black pepper. Moreover, BCP is found in copaiba (*Copaifera spp.*) and marijuana/hemp (*Cannabis spp.*), which have been used in traditional medicine for centuries due to their anti-inflammatory and analgesic effects (Gertsch *et al.*, 2010). Due to its favorable taste and scent and apparent lack of toxicity, BCP is approved by the FDA as a food additive for flavoring. BCP, which is devoid of psychoactive effects, has been demonstrated to activate cannabinoid 2 receptors (CB2), which are primarily expressed in immune and immune-derived cells. This makes BCP a promising food-derived agent that may be exploited therapeutically to treat various inflammatory diseases (Gertsch *et al.*, 2008). BCP has been reported to exert protective effects in experimental animal models of inflammatory pain (Gertsch *et al.*, 2008), kidney injury (Horvath *et al.*, 2012b), ischemic stroke (Choi *et al.*, 2013), Parkinson`s disease (Ojha *et al.*, 2016), toxic hepatitis (D-galactosamine- and endotoxin-induced) (Cho *et al.*, 2015), experimental liver fibrosis (Mahmoud *et al.*, 2014), and colitis (Bento *et al.*, 2011). BCP has been also proposed recently, to exert anti-addictive potential (Al Mansouri *et al.*, 2014). BCP has been reported to act on targets other than CB2, involving SIRT-1 (Zheng *et al.*, 2013), PPAR-α (Wu *et al.*, 2014), FAAH, or COX-2 (Chicca *et al.*, 2014).

Endocannabinoids and cannabinoid receptor signaling play a central role in the development of liver diseases by influencing pivotal inflammatory and metabolic pathways (Silvestri *et al.*, 2013; Tam *et al.*, 2011; Teixeira-Clerc *et al.*, 2010). Activation of hepatic cannabinoid 1 receptor (CB1) by endocannabinoids or synthetic ligands promotes alcoholic- (Jeong *et al.*, 2008) and non-alcoholic steatohepatitis (Osei-Hyiaman *et al.*, 2005; Tam *et al.*, 2012), liver injury (Cao *et al.*, 2013; Horvath *et al.*, 2012a) and fibrosis (Teixeira-Clerc *et al.*, 2006). In contrast, CB2 receptor activation has tissue protective, anti-inflammatory and antifibrotic effects in preclinical models of liver injury, inflammation and fibrosis (Batkai *et al.*, 2007; Cao *et al.*, 2013; Horvath *et al.*, 2012a; Louvet *et al.*, 2011; Teixeira-Clerc *et al.*, 2010). However, despite the promise of selective CB2 receptor agonists in liver disease based on preclinical studies, no CB2 agonists are available suitable for human testing in liver disease to date. Unlike the potent synthetic CB2 receptor agonists currently used in animal models, the phytochemical BCP could be more readily tested in humans as it is a FDA approved food additive, thus having immediate translational potential.

Accepted Article

This article is protected by copyright. All rights reserved.

Inflammation plays a crucial role in the development and progression of alcoholic liver disease. In this study, we investigated if BCP treatment exerts beneficial effects against liver injury and inflammation induced by chronic plus binge ethanol feeding, and whether these effects were mediated via CB2 receptors.

Materials and Methods

Animals and Chemicals

All the animal protocols conformed to the National Institutes of Health (NIH) guidelines and were approved by the Institutional Animal Care and use Committee of the National Institute on Alcohol Abuse and Alcoholism (Bethesda, MD). The experiments were complied with BJP Policy on reporting experiments involving animals and with the principles of ARRIVE guidelines. 10-week-old male C57BL/6J mice were obtained from the Jackson Laboratory (Bar Harbor, ME). Male $CB2^{-/-}$ mice on C57BL/6J background and their wild-type controls ($CB2^{+/+}$) were used in the study (termed $CB2^{-/-}$ and $CB2^{+/+}$ mice).

(*E*)-beta-caryophyllene (BCP) was obtained as previously described (Gertsch *et al.*, 2008). Analytical measurements by GC-MS showed that it was 95% pure with beta-caryophylelne oxide and alpha-humulene as the major impurities.

Alcoholic Steatohepatitis Model

Male C57BL/6J mice, weighing more than 20 g were used for ad libitum ethanol feeding, as described as the chronic plus binge alcohol feeding-induced steatohepatitis model used and developed at the NIAAA (Bertola *et al.*, 2013a). Lieber-DeCarli ‘82 Shake and Pour control liquid diet (Bio-Serv, product no. F1259SP) and Lieber-DeCarli ‘82 Shake and Pour ethanol liquid diet (Bio-Serv, product no. F1258SP) were used for diet preparation. Mice were fed liquid control diet (Bio-Serv, Frenchtown, NJ) for 5 days, and from day 5 mice were switched either to a liquid diet containing 5% ethanol for 10 days, or were pair-fed a control diet for 10 days. BCP (10mg/kg dose dissolved in DMSO-Tween-Saline in a ratio of 1:1:18) or vehicle were administered intraperitoneally every day. At day 11, mice in the ethanol groups were gavaged with a single dose of ethanol (5 g/kg body weight, 30% ethanol), whereas the mice in the control groups were gavaged with isocaloric maltodextrin solution. All mice were sacrificed 9 h after gavage.

This article is protected by copyright. All rights reserved.

Determination of BCP Pharmacokinetics In Vivo

We studied the pharmacokinetic properties of BCP, in two set of experiments. To test the effect of chronic BCP treatment and the potential influence of ethanol feeding, in a separate set of experiments, BCP (10mg/kg/day dose dissolved in DMSO-Tween-Saline in a ratio of 1:1:18) or vehicle were administered intraperitoneally to male C57BL/6J mice for 10 days in accordance with our Lieber-DeCarli ethanol feeding protocol, described above. After the administration of the last dose of BCP, liver, brain and serum samples were collected at 30, 60, 120, and 360 min time points.

In a separate set of experiment BCP (10mg/kg single dose dissolved in DMSO-Tween-Saline in a ratio of 1:1:18) or vehicle were administered intraperitoneally or orally to male C57BL/6J mice and serum samples were collected at 30, 60, 120, and 360 min after drug administration.

BCP was quantified in liver, kidney, brain and serum. Snap-frozen tissues were weighted and transferred into a 2 ml tube containing 3 chrome-steel beads and 0.1 M formic acid and homogenized using a mini bead beater (except for the serum). An aliquot of the homogenized tissues (100 µl) was rapidly transferred into plastic tube containing 90 µl of ethyl acetate and 10 µl of α-humulene (used as internal standard), strongly vortexed for 30 seconds and sonicated in ice-cold bath for 5 min. Then, samples were centrifuged at max speed for 10 min at 4°C and kept for 1 h at -20°C to facilitate the recovery of the upper organic phase. Samples were analyzed by gas chromatography (GC)/electron ionization (EI)-mass spectrometry using an Agilent 6890 N GC equipped with a 30 m HP-5MS column and a 5975 C EI-MS with triple-axis detector. As carrier gas, helium was used at a constant flow rate of 1.0 ml/min with splitless injection. Separation of BCP and its internal standard was achieved with the following oven program: initial temp. of 100 °C followed by an increase to 120 °C at 15 °C/min, kept for 0.5 min before increasing to 180°C at 7 °C/min. Oven temperature was finally increased to 310°C at 20 °C/min for a total time of 18.9 min. The following specific ions were used for selected ion monitoring: m/z 93 for α-humulene and m/z 91 for BCP.

Determination of Liver Injury

After venous blood collection, serum was prepared (centrifugation for 10 min at 2500 G) immediately followed by the determination of the serum levels of alanine aminotransferase (ALT) using a clinical chemistry analyzer - Idexx VetTest 8008 (Idexx Laboratories, Westbrook, ME, USA).

Reverse Transcription and Real-Time PCR

This article is protected by copyright. All rights reserved.

Hepatic tissues were homogenized in Trizol (Invitrogen, Carlsbad, CA, USA) and total RNA was isolated with Direct-zol™ RNA MiniPrep Kit (Zymo Research, Irvine, CA, USA). All RNA samples have been DNAse digested, and RNA concentration have been measured with NanoDrop (Thermo Scientific, Waltham, MA USA). 2 µg RNA was' reverse-transcribed (High-Capacity cDNA Reverse Transcription Kit, Applied Biosystems, Foster City, CA, USA) and the target genes were amplified using the standard SyberGreen based real-time PCR kit (SYBR® Select Master Mix, Applied Biosystems, Foster City, CA). Primers sequences are provided in Supplementary Table 1.

Histology and Immunohistochemistry

After routine FFPE specimen processing, 5 µm thick liver sections were prepared and stained with hematoxylin and eosin (H&E) for histological evaluation of liver injury.

For immunohistochemistry, deparaffinized sections underwent antigen retrieval (pH=6 citrate buffer, at 95 ^{0}C for 10 min or Proteinase K (20µg/ml in Tris-EDTA buffer pH=8) digestion for F4/80 staining, at 37 ^{0}C for 15 min followed by 10 min additional digestion at room temperature). After blocking endogenous peroxidase activity (3% H_2O_2 solution in PBS), the sections were blocked in appropriate sera (2.5% goat, or horse serum in PBS and 2% milk powder or bovine serum albumin). Primary antibodies (4-HNE (Japan Institute for the Control of Aging, Nikken SEIL Co., Fukuroi, Shizuoka, Japan), Iba-1 (Wako Pure Chemical Industries, Chuo-Ku, Osaka, Japan), F4/80 (eBioscience, San Diego, CA, USA), Ly6-G (Abcam, Cambridge, MA, USA)) were incubated with the sections overnight in diluted blocking solution at 4 ^{0}C. After primary antibody incubations, the sections were washed three times in PBS and incubated for an hour either with biotinylated secondary antibody (Vectastain ABC kit, Vector Laboratories, Burlingame, CA, USA) or with an anti-rat IgG/anti-rabbit IgG conjugated with a peroxidase polymer (ImmPress reagents, Vector Laboratories, Burlingame, CA, USA). Secondary antibodies were washed 3 times for 10 min and the specific signal was developed with diaminobenzidine (ImmPACT DAB EqV Peroxidase (HRP) Substrate, Vector Laboratories, Burlingame, CA, USA). The specific staining was visualized and images were acquired using BX-41 microscope (Olympus, Tokyo, Japan).

For confocal imaging, the sections were incubated with a goat anti-rabbit IgG secondary antibody, conjugated to Alexa Fluor® 594 or Alexa Fluor® 488 (Thermo Scientific, Waltham, MA USA). Nuclei were stained with the far-red emitting DRAQ5 stain (Cell Signaling Technology, Danvers, MA, USA) and visualized under a Zeiss LSM710 confocal microscope (Jena, Germany).

This article is protected by copyright. All rights reserved.

Accepted Article

Liver samples embedded in optimal cutting temperature (OCT) compound were cut (10 µm) and stained with Oil Red O (Sigma-Aldrich, St. Louis, MO, USA) dissolved in isopropanol to evaluate hepatic lipid accumulation.

Determination of Hepatic Triglyceride Content

Triglyceride content was measured from frozen liver tissues by the Triglyceride Quantification Colorimetric Kit (Biovision, San Francisco, CA, USA) according to the manufacturer's instructions.

Determination of Hepatic Endocannabinoid Content

Endocannabinoids were measured from frozen liver tissues by stable isotope dilution liquid chromatography/tandem mass spectrometry (LC-MS/MS) as described previously (Mukhopadhyay *et al.*, 2011)

Western Blots

Frozen liver samples were homogenized in RIPA lysis buffer (150 mM NaCl, 50 mM Tris, 1%NP-40). Protein concentrations were determined by means of bicinchoninic acid method using bovine serum albumin as standard (Pierce, Rockford, USA). 20 µg of protein was loaded from each sample onto 4-20% polyacrylamide gel. After separation by electrophoresis, proteins were transferred (Trans-Blot Turbo Blotting System, BioRad, Hercules, CA, USA) onto the PVDF membrane. Successful transfer was controlled by using Ponceau dye. The membrane was blocked with 5% non-fat dry milk in 0.05% TBS-T for 1 hour at room temperature. After the blocking step, the membrane was incubated with a primary antibody (dissolved in 1% non-fat dry milk–TBS-T, 1:1000 dilution) against either SIRT-1 (Cell Signaling Technology, Danvers, MA, USA), PPAR-α (Abcam, Cambridge, MA, USA), or Acetyl-Lysine (Cell Signaling Technology, Danvers, MA, USA) for 2 h at room temperature, followed by washing with 0.05% TBS-T (3 × 10 min). After washing, the membrane was incubated with a secondary antibody (horseradish peroxidase-conjugated affinity purified goat anti-rabbit, 1/5000 dilution) in 1% non-fat dry milk in TBS-T for 1 h at room temperature. Then the membrane was washed again 3 times for 10 min. For detection of the bands, the membrane was incubated with ECL reagent (SuperSignal West Pico Substrate, Thermo Scientific - Pierce, Rockford, IL, USA) for 5 min and the signal was recorded in a gel documentation system (Versadoc 4000MP, Bio-Rad Imaging System, Hercules, USA). Band densities were evaluated by using Quantity One software (Bio-Rad Imaging System, Hercules, USA). Loading control was done by determining the actin content of each sample. Briefly, after stripping the membrane, it was probed with a primary antibody directly conjugated with HRP that recognizes actin (1/10,000 dilution - Abcam, Cambridge,

This article is protected by copyright. All rights reserved.

Accepted Article

MA, USA) for 1 h at room temperature, followed by washing with TBS-T. Actin band visualization and evaluation of band densities were done as described above. There was no significant difference in actin between the groups.

Statistical Analysis

All the values are represented as mean ± SEM. Statistical analysis of the data was performed by one or two-way analysis of variance (ANOVA) followed by Tukey's post-hoc test for multiple comparisons, as appropriate. The analysis was conducted using GraphPad-Prism4 software. $P < 0.05$ was considered statistically significant.

Accepted Article

This article is protected by copyright. All rights reserved.

Results

β-caryophyllene treatment protects against alcoholic steatohepatitis

We aimed to study the potential hepatoprotective action of BCP in setting of alcoholic liver disease. We employed the chronic plus binge ethanol feeding model, developed in the National Institute on Alcohol Abuse and Alcoholism (Bertola *et al.*, 2013a), resembling major pathologic features of early alcoholic liver disease, involving hepatocyte injury, pro-inflammatory alterations, and steatosis. BCP was administered daily during the course of Liber-DeCarli alcohol feeding protocol and at the end of the feeding period it was given 1 hour prior to binge ethanol treatment (**Fig.1. A**). BCP treatment significantly alleviated binge alcohol-induced liver injury, as reflected by a decrease in serum ALT levels (**Fig.1. B**), and normalized the histopathological signs of alcoholic steatohepatitis (ballooning of hepatocytes, microvesicular steatosis, and neutrophil inflammatory infiltrates/loci) (**Fig.1. C**), and attenuated oxidative tissue injury, as reflected by reduced amount of 4-hydroxy-nonenal accumulation (**Fig. 1. D**).

β-caryophyllene treatment prevents the pro-inflammatory phenotypic switch of hepatic macrophages upon chronic plus binge ethanol feeding

Hepatic macrophage population undergoes a major phenotypic switch during the course of alcohol feeding (Wang *et al.*, 2014). In a healthy control liver, a mixed population of larger and smaller Kupffer cell population is present: larger, spindle-shaped peri-sinusoidal macrophages are involved in phagocytosis and are less prone to activation, while the smaller, round-shaped peri-central macrophage population is more prone to activation and pro-inflammatory cytokine and reactive oxygen species production (Laskin *et al.*, 2001). To characterize macrophage morphology, we employed the pan-macrophage marker ionized calcium-binding adapter molecule (Iba-1) (Rehg *et al.*, 2012). As an actin cross-linking protein, being involved in cytoskeletal reorganization, immunohistochemical detection of Iba-1 gives a sharp and detailed picture of macrophage morphology (**Fig. 2. A**) (Kohler, 2007) in comparison to staining for cell membrane-specific markers F4/80 or CD68 (**Fig. 2. B and Supplementary Fig. 1.**). Accordingly, we detected the presence of the large Kupffer cells along the hepatic sinuses with arborized morphology both in the vehicle and BCP treated pair-fed groups (**Fig. 2. A**). However, upon ethanol-feeding we detected small, round-shaped macrophages with less arborized morphology, resembling `M1`-type of morphology. BCP treatment partially prevented this morphological switch: large macrophages with arborization were present along the hepatic sinusoids (**Fig. 2. A and B**).

This article is protected by copyright. All rights reserved.

Accepted Article

In line with the above observations, mRNA markers of tissue-resident macrophages, F4/80, CD68, and Iba-1 were down-regulated due to chronic plus binge ethanol feeding, an effect that was mitigated by BCP treatment (**Fig.3. A**). In addition CD11b expression, a marker of pro-inflammatory lymphocytes (mainly monocytes and macrophages) showed a striking increase in the ethanol-fed groups, that was attenuated by BCP treatment (**Fig.3. A**).

Ethanol-fed mice displayed significant induction of `M1` markers of macrophage activation, including IL1ß, IL-6 and the chemokines, chemokine ligand 2 (CCL2 – MCP-1), and CXCL-2 (MIP-2). In addition, there was also a parallel induction of genes characteristic of an alternative `M2` activation signature, such as upregulation of arginase 1 (Arg1) and cluster of differentiation 163 (CD163), both attenuated by BCP treatment (**Fig.3. B**). Other markers of `M2` activation, like mannose receptor C type 2 (Mrc2), macrophage galactose-type C-type lectin 1 (MGL1/CD301), C-type lectin domain family 7 member A (Clec7a), and IL-10 showed down-regulation, that was attenuated by BCP treatment only in the case of IL-10 (**Fig.3. C**). These findings show that chronic alcohol feeding promotes polarization of Kupffer cells toward a mixed M1/M2 phenotype, an effect that is minimized by BCP treatment mainly in the case of `M1` activation.

β-caryophyllene treatment prevents vascular inflammation and subsequent hepatic neutrophil infiltration due to chronic plus binge ethanol feeding

Neutrophil infiltration is a key pathologic finding in alcoholic hepatitis and has been shown to closely correlate with the severity of alcoholic hepatic injury (Bertola *et al.*, 2013b; Dominguez *et al.*, 2009). Immunohistochemical staining for the neutrophil marker Ly6G confirmed that a large number of neutrophils had infiltrated the livers of chronic plus binge ethanol-fed mice, compared with control pair-fed mice. This effect of ethanol feeding was largely attenuated by BCP treatment (**Fig. 4. A and B**). Chronic plus binge ethanol feeding also led to a marked up-regulation of hepatic mRNA expression of the neutrophil marker, Ly6G (**Fig. 4. C**).

To further investigate how chronic plus binge ethanol feeding leads to infiltration of neutrophils into the liver, hepatic expression of several vascular and tissue adhesion molecules were examined, reflecting vascular inflammatory processes. Chronic plus binge ethanol feeding resulted in the induction of ICAM-1, E-selectin, and P-selectin, which were significantly attenuated by BCP treatment (**Fig. 4. D**).

This article is protected by copyright. All rights reserved.

β-caryophyllene treatment prevents alcoholic steatosis and preserves PPAR-α-dependent signaling

Daily administration of BCP prevented ethanol-feeding-induced development of microvesicular steatosis, as shown by oil red o staining on fresh frozen liver sections (**Fig. 5. A**). Quantification of liver triglycerol content confirmed the beneficial effect of BCP treatment on alcohol-induced hepatic lipid accumulation (**Fig. 5. B**). Since BCP and its metabolites have been proposed to affect cyclooxygenase-2 (COX2) and fatty acid amide hydrolase (FAAH) activity (Chicca *et al.*, 2014), we aimed to measure endocannabinoids and related lipids in pair-fed mice treated either with vehicle or BCP (10 mg/kg). None of the measured lipids showed changes due to BCP treatment (anandamide: 0.90±0.06 fmol/mg in vehicle vs. 1.12±0.18 fmol/mg in BCP treated livers; 2-arachidonoylglycerol: 1.43±0.23 pmol/mg in vehicle vs. 1.41±0.46 pmol/mg in BCP treated livers; oleoylethanolamide: 13.66±1.38 fmol/mg in vehicle vs. 15.56±1.98 fmol/mg in BCP treated livers; arachidonic acid: 0.53±0.03 pmol/mg in vehicle vs. 0.41±0.12 pmol/mg in BCP treated livers), implicating that the hepatoprotective effect of BCP is not related to COX2 or FAAH inhibition.

Ethanol metabolism results in increased acetyl-CoA formation, with concomitant protein-acetylation and thereby leading to reprogramming of intermedier metabolism (Shepard *et al.*, 2009). Sirtuins (SIRT) are NAD^+-dependent protein deacetylase enzymes, capable of removing acetyl groups from proteins, and thereby preventing the development of alcoholic (Yin *et al.*, 2014) and non-alcoholic fatty liver disease (Li *et al.*, 2014). In line with these, we detected an increase in overall lysine acetylation in chronic plus binge ethanol-fed group that was attenuated by BCP treatment (**Fig. 6. A**). The increased acetylation pattern seen in ethanol-fed livers was paralleled by a decrease in SIRT-1 protein level, however, SIRT-1 expression seems to be not influenced by BCP treatment.

We detected a massive reduction both in protein (**Fig. 6. B**) and mRNA levels of PPAR-α (**Fig. 6. C**) due to ethanol feeding, which was mitigated by BCP treatment. In line with this observation BCP treatment preserved the expression of PPAR-α-related mRNA targets (peroxisome proliferator-activated receptor gamma coactivator 1- beta - PGC-1ß, glucose-6-phosphatase – G6PC, phosphoenolpyruvate carboxykinase 1 - Pck1, phosphofructokinase - PFK, and 3-hydroxy-3-methylglutaryl-CoA synthase 2 – HMGCS2) upon chronic plus binge ethanol feeding (**Fig. 6. D and E**). Interestingly, we detected a massive ethanol-feeding-induced up-regulation of a known PPAR-α target gene, the

This article is protected by copyright. All rights reserved.

fibroblast growth factor 21 (FGF21). However, this effect was markedly attenuated by BCP treatment (**Fig. 6. F**)

The beneficial effects of β-caryophyllene treatment against alcoholic steatosis are attenuated in CB2 deficient mice

Since BCP has been proposed to act on potential targets (SIRT-1, PPAR-α , COX-2) other than CB2 receptor, we aimed to test, if there is any protective effect of BCP treatment in CB2 receptor deficient mice. We were not able to detect any marked effect of BCP treatment on macrophage morphology in ethanol-fed CB2 deficient mice (**Fig. 7. A**). This was further substantiated by the analysis of expression of F4/80 and CD11b, which were not affected by BCP treatment in CB2 knock-out mice (**Fig. 7. B**).

We observed mild steatosis even in control pair-fed CB2 deficient mice. There was a significant induction of microvesicular steatosis in ethanol-fed CB2 deficient mice, however, this was not affected by BCP treatment (**Fig. 7. C**). On examining PPAR-α expression and PPAR-α -related targets, we saw that effects observed in wild type ethanol-fed and BCP treated mice were lost in CB2 deficient mice (**Fig. 7. D**).

Pharmacokinetic properties of β-caryophyllene

BCP reached comparable serum (**Fig.8. A**), hepatic (**Fig.8. B**) and brain levels (**Fig.8. C**) in both ethanol-fed and pair-fed animals. BCP tissue concentrations indicated a 50-fold higher distribution in liver compared to brain. In addition BCP showed good oral bioavailability in comparison to the used intraperitoneal administration (**Fig.8. D**).

Discussion

In the present study we demonstrate that treatment with the dietary phytochemical BCP exerts marked hepatoprotective effects in the setting of chronic liver injury induced by chronic and binge alcohol feeding in mice. We show that 1) in the chronic and binge alcohol-induced liver injury model BCP attenuates the pro-inflammatory phenotypic `M1` switch of Kupffer cells and 2) BCP treatment reduces expression of tissue and vascular adhesion molecules ICAM-1, E-Selectin and P-Selectin, as well as consequent neutrophil infiltration; 3) BCP beneficially influences alcohol-induced hepatic metabolic dysregulation (steatosis, protein hyperacetylation, and PPAR-α signaling); 4) these protective effects of BCP involve CB2 receptor activation.

CB2 is primarily expressed on immune and immune derived cells, including the Kupffer cells of the liver (Cao *et al.*, 2013; Pacher *et al.*, 2011; Teixeira-Clerc *et al.*, 2010).

This article is protected by copyright. All rights reserved.

Activation of CB2 receptors mediate anti-inflammatory actions, limiting inflammatory and subsequent oxidative/nitrative tissue injury and organ damage (Pacher *et al.*, 2011).

Resident macrophages of the liver (Kupffer cells), account approximately for 10–15% of all liver cells. These cells are localized along the sinusoidal space of Disse anchored to endothelial cells by long cytoplasmic processes, being involved in maintaining tissue homeostasis and providing immunosurveillance. In addition, they also play a protective role in promoting liver regeneration (Meijer *et al.*, 2000). Kupffer cells may become activated by a variety of stimuli that trigger innate immunity, involving endogenous molecules released during hepatocyte injury (e.g. hyaluronic acid, heparin sulfate, high-mobility group box 1 (HMGB1), or heat shock proteins) (Tsung *et al.*, 2005). In addition, Kupffer cell activation might be triggered by environmental toxins, as in the case of alcoholic steatohepatitis by ethanol and its metabolites or by endotoxin, absorbed due to increased gastrointestinal permeability. Pathologically over-activated macrophages, as seen in alcoholic-, and in non-alcoholic fatty liver disease, may further aggravate tissue injury and inflammation, leading to liver failure. Since BCP has been proposed to protect the colonic mucosa against dextran sulfate-induced colitis (Bento *et al.*, 2011; Cho *et al.*, 2007), it is possible that BCP exert similar protection against ethanol-induced mucosal damage and thereby also attenuates endotoxin translocation from the gut to the portal circulation (Bode *et al.*, 1987).

Kupffer cells consist of three major different subsets; the $CD11b^+$ cells, and $CD68^+$ cells overlapping with $CD32^+$ cells, representing precursors of CD68+ cells (expressing stem cell markers, such as c-kit (CD117) and CD34 (Kinoshita *et al.*, 2010). Detailed flow cytometric and immunohistochemical studies also revealed that the $CD68^+$ cells are large and spindle-shaped, while the $CD11b^+$ cells are small and round or oval-shaped (Ikarashi *et al.*, 2013). While large macrophages are more phagocytic and generate increased quantities of lysosomal enzymes, the smaller macrophages release more reactive oxygen species, and appear to be more susceptible to `M1`-type of activation and cytokine production. Interestingly, we found that chronic and binge alcohol feeding resulted in pro-inflammatory phenotypic switch in liver Kupffer cells, which was attenuated by BCP treatment.

Experimental CB2 agonists (e.g.: JWH-133, HU910, HU308) have been shown to favorably affect overall hepatic macrophage activation upon chronic alcohol exposure (Louvet *et al.*, 2011) and hepatocyte injury (Batkai *et al.*, 2007; Horvath *et al.*, 2012a; Rajesh *et al.*, 2008). However, not a single CB2 agonist is approved for clinical testing in liver disease yet. In this study, we demonstrate that the FDA approved food additive BCP, which is present in various food and medicinal plants, as well as in cannabis essential oil, exerts

This article is protected by copyright. All rights reserved.

Accepted Article

hepatoprotective effects in a model of alcohol-induced chronic liver injury. The observed protective effects were attenuated in CB2 knockout mice indicating involvement of CB2. To increase the translational potential of our study, we also tested the pharmacokinetic properties of oral and intraperitoneal BCP administration both in healthy and in ethanol-fed mice. BCP was orally bioavailable, and ethanol-feeding did not interfere with its kinetics (e.g. absorption, or metabolism). The BCP dose used in our study in mice (10 mg/kg) is convertible to a human equivalent dose of approximately 0.8-1 mg/kg/day for adult human subjects (Nair *et al.*, 2016). Based on the mouse pharmacokinetics data, repeated oral dosing of BCP might be desirable, the benefit of which remains to be tested.

Our results also suggest that BCP has beneficial properties on intermediary metabolism in ethanol-fed animals, potentially by decreasing pro-inflammatory cytokine expression in a CB2-dependent manner and thereby preserving PPAR-α -related signaling that is characteristic for the healthy liver.

An intriguing field of investigation is how pro-inflammatory alterations influence hepatic intermediary metabolism. It is now well established that pro-inflammatory cytokines (IL-1ß or TNFα) may profoundly affect hepatic lipid and glucose metabolism in a paracrine manner (Louvet *et al.*, 2011; Stienstra *et al.*, 2010). Stienstra et al. has shown that IL-1ß is capable to suppress human and mouse PPAR-α promoter activity and in parallel interferes with the ability of PPAR-α to activate transcription of target genes (Stienstra *et al.*, 2010). We found that alcohol markedly impaired PPAR-α signaling and increased lipid accumulation in the liver, which were significantly attenuated by BCP treatment, however, the effects seem to relate to BCP-induced CB2 activation rather than to a direct PPAR-α mediated effect.

During hepatic ethanol metabolism, liver mitochondria convert acetate into acetyl-CoA that is further processed in the citric acid cycle. However, due to ethanol metabolism, there is an increased level of NADH that inhibits further metabolism of the acetyl-CoA by the citric acid cycle. In addition excess NADH inhibits gluconeogenesis by preventing the oxidation of lactate to pyruvate, leading to accumulation of lactate (lactic acidosis), and causing hypoglycemia (Tsai *et al.*, 2015). Further consequences of hepatic acetyl-CoA accumulation involves increased protein acetylation (histones, transcription factors – SREBP1c, FOXO1, FOXO3, PGC1α - (Shepard *et al.*, 2009)), ketone body formation, increased fatty acid synthesis and fat storage, and buildup of acetaldehyde. Increased production of acetaldehyde forms covalent bonds with many important functional groups in proteins, impairing protein function. It may also react with phospholipids and arachidonic

This article is protected by copyright. All rights reserved.

Accepted Article

acid, which triggers lipid peroxidation reactions promoting hepatocyte cell death. Consistently with the above, we found increased protein acetylation and lipid peroxidation (4HNE formation) in livers of ethanol-fed groups, which were attenuated by BCP treatment. Collectively, our results demonstrate that BCP treatment exerts beneficial effects against liver injury induced by chronic plus binge ethanol feeding by attenuating the Kupffer cell-mediated pro-inflammatory response (activation and/or pro-inflammatory phenotypic `M1` switch), neutrophil-mediated oxidative/nitrative stress/injury, vascular inflammation (expression of vascular adhesion molecules), and hepatic metabolic dysregulation (steatosis, protein hyperacetylation, and PPAR-α signaling). Our results also indicate that these in vivo protective effects of BCP against alcohol-induced hepatic injury may involve, at least in part, CB2 mediated mechanisms. Our study may have immediate translational potential in liver disease since BCP is an FDA approved food additive in humans.

Author Contributions

Z.V.V., P.P. conception and design of research; Z.V.V., C.M., K.E., R.C., D.N., A.C., B.T.N., J.P., T.L., L.C. performed experiments; Z.V.V., C.M., A.C., J.P., and B.T.N. analyzed data; Z.V.V., R.C., G.H., A.C., B.G., G.K., J.G., and P.P. interpreted results of experiments; Z.V.V. and P.P. prepared figures; Z.V.V and P.P. drafted manuscript; Z.V.V., A.C., G.H., B.G.,G.K., J.G., and P.P. edited and revised manuscript; Z.V.V., C.M., K.E., R.C., D.N., A.C., B.T.N., J.P., T.L., L.C., G.H., B.G.,G.K., J.G., and P.P. approved final version of manuscript.

Acknowledgments

The recent work was supported by the Intramural Research Program of NIAAA/NIH (to P. Pacher). C. Matyas was supported by the scholarship of the Hungarian-American Enterprise Scholarship Fund/Council on International Educational Exchange. Z. V. Varga was supported by the Rosztoczy Foundation.

Accepted Article

This article is protected by copyright. All rights reserved.

References

Al Mansouri S, Ojha S, Al Maamari E, Al Ameri M, Nurulain SM, Bahi A (2014). The cannabinoid receptor 2 agonist, beta-caryophyllene, reduced voluntary alcohol intake and attenuated ethanol-induced place preference and sensitivity in mice. *Pharmacology, biochemistry, and behavior* **124:** 260-268.

Batkai S, Osei-Hyiaman D, Pan H, El-Assal O, Rajesh M, Mukhopadhyay P*, et al.* (2007). Cannabinoid-2 receptor mediates protection against hepatic ischemia/reperfusion injury. *FASEB journal : official publication of the Federation of American Societies for Experimental Biology* **21**(8)**:** 1788-1800.

Bento AF, Marcon R, Dutra RC, Claudino RF, Cola M, Leite DF*, et al.* (2011). beta-Caryophyllene inhibits dextran sulfate sodium-induced colitis in mice through CB2 receptor activation and PPARgamma pathway. *The American journal of pathology* **178**(3)**:** 1153-1166.

Bertola A, Mathews S, Ki SH, Wang H, Gao B (2013a). Mouse model of chronic and binge ethanol feeding (the NIAAA model). *Nature protocols* **8**(3)**:** 627-637.

Bertola A, Park O, Gao B (2013b). Chronic plus binge ethanol feeding synergistically induces neutrophil infiltration and liver injury in mice: a critical role for E-selectin. *Hepatology* **58**(5)**:** 1814-1823.

Bode C, Kugler V, Bode JC (1987). Endotoxemia in patients with alcoholic and non-alcoholic cirrhosis and in subjects with no evidence of chronic liver disease following acute alcohol excess. *Journal of hepatology* **4**(1)**:** 8-14.

Cao Z, Mulvihill MM, Mukhopadhyay P, Xu H, Erdelyi K, Hao E*, et al.* (2013). Monoacylglycerol lipase controls endocannabinoid and eicosanoid signaling and hepatic injury in mice. *Gastroenterology* **144**(4)**:** 808-817 e815.

Chicca A, Caprioglio D, Minassi A, Petrucci V, Appendino G, Taglialatela-Scafati O*, et al.* (2014). Functionalization of beta-caryophyllene generates novel polypharmacology in the endocannabinoid system. *ACS chemical biology* **9**(7)**:** 1499-1507.

Cho HI, Hong JM, Choi JW, Choi HS, Kwak JH, Lee DU*, et al.* (2015). beta-Caryophyllene alleviates D-galactosamine and lipopolysaccharide-induced hepatic injury through suppression of the TLR4 and RAGE signaling pathways. *European journal of pharmacology* **764:** 613-621.

Cho JY, Chang HJ, Lee SK, Kim HJ, Hwang JK, Chun HS (2007). Amelioration of dextran sulfate sodium-induced colitis in mice by oral administration of beta-caryophyllene, a sesquiterpene. *Life sciences* **80**(10)**:** 932-939.

Choi IY, Ju C, Anthony Jalin AM, Lee DI, Prather PL, Kim WK (2013). Activation of cannabinoid CB2 receptor-mediated AMPK/CREB pathway reduces cerebral ischemic injury. *The American journal of pathology* **182**(3)**:** 928-939.

Dominguez M, Miquel R, Colmenero J, Moreno M, Garcia-Pagan JC, Bosch J*, et al.* (2009). Hepatic expression of CXC chemokines predicts portal hypertension and survival in patients with alcoholic hepatitis. *Gastroenterology* **136**(5)**:** 1639-1650.

This article is protected by copyright. All rights reserved.

Gertsch J, Leonti M, Raduner S, Racz I, Chen JZ, Xie XQ*, et al.* (2008). Beta-caryophyllene is a dietary cannabinoid. *Proceedings of the National Academy of Sciences of the United States of America* **105**(26)**:** 9099-9104.

Gertsch J, Pertwee RG, Di Marzo V (2010). Phytocannabinoids beyond the Cannabis plant - do they exist? *British journal of pharmacology* **160**(3)**:** 523-529.

Horvath B, Magid L, Mukhopadhyay P, Batkai S, Rajesh M, Park O*, et al.* (2012a). A new cannabinoid CB2 receptor agonist HU-910 attenuates oxidative stress, inflammation and cell death associated with hepatic ischaemia/reperfusion injury. *British journal of pharmacology* **165**(8)**:** 2462-2478.

Horvath B, Mukhopadhyay P, Kechrid M, Patel V, Tanchian G, Wink DA*, et al.* (2012b). beta-Caryophyllene ameliorates cisplatin-induced nephrotoxicity in a cannabinoid 2 receptor-dependent manner. *Free radical biology & medicine* **52**(8)**:** 1325-1333.

Ikarashi M, Nakashima H, Kinoshita M, Sato A, Nakashima M, Miyazaki H*, et al.* (2013). Distinct development and functions of resident and recruited liver Kupffer cells/macrophages. *Journal of leukocyte biology* **94**(6)**:** 1325-1336.

Jeong WI, Osei-Hyiaman D, Park O, Liu J, Batkai S, Mukhopadhyay P*, et al.* (2008). Paracrine activation of hepatic CB1 receptors by stellate cell-derived endocannabinoids mediates alcoholic fatty liver. *Cell metabolism* **7**(3)**:** 227-235.

Kinoshita M, Uchida T, Sato A, Nakashima M, Nakashima H, Shono S*, et al.* (2010). Characterization of two F4/80-positive Kupffer cell subsets by their function and phenotype in mice. *Journal of hepatology* **53**(5)**:** 903-910.

Kohler C (2007). Allograft inflammatory factor-1/Ionized calcium-binding adapter molecule 1 is specifically expressed by most subpopulations of macrophages and spermatids in testis. *Cell and tissue research* **330**(2)**:** 291-302.

Laskin DL, Weinberger B, Laskin JD (2001). Functional heterogeneity in liver and lung macrophages. *Journal of leukocyte biology* **70**(2)**:** 163-170.

Li Y, Wong K, Giles A, Jiang J, Lee JW, Adams AC*, et al.* (2014). Hepatic SIRT1 attenuates hepatic steatosis and controls energy balance in mice by inducing fibroblast growth factor 21. *Gastroenterology* **146**(2)**:** 539-549 e537.

Louvet A, Teixeira-Clerc F, Chobert MN, Deveaux V, Pavoine C, Zimmer A*, et al.* (2011). Cannabinoid CB2 receptors protect against alcoholic liver disease by regulating Kupffer cell polarization in mice. *Hepatology* **54**(4)**:** 1217-1226.

Mahmoud MF, Swefy SE, Hasan RA, Ibrahim A (2014). Role of cannabinoid receptors in hepatic fibrosis and apoptosis associated with bile duct ligation in rats. *European journal of pharmacology* **742:** 118-124.

Meijer C, Wiezer MJ, Diehl AM, Schouten HJ, Schouten HJ, Meijer S*, et al.* (2000). Kupffer cell depletion by CI2MDP-liposomes alters hepatic cytokine expression and delays liver regeneration after partial hepatectomy. *Liver* **20**(1)**:** 66-77.

This article is protected by copyright. All rights reserved.

Mukhopadhyay B, Cinar R, Yin S, Liu J, Tam J, Godlewski G*, et al.* (2011). Hyperactivation of anandamide synthesis and regulation of cell-cycle progression via cannabinoid type 1 (CB1) receptors in the regenerating liver. *Proceedings of the National Academy of Sciences of the United States of America* **108**(15)**:** 6323-6328.

Nair AB, Jacob S (2016). A simple practice guide for dose conversion between animals and human. *Journal of basic and clinical pharmacy* **7**(2)**:** 27-31.

Ojha S, Javed H, Azimullah S, Haque ME (2016). beta-Caryophyllene, a phytocannabinoid attenuates oxidative stress, neuroinflammation, glial activation, and salvages dopaminergic neurons in a rat model of Parkinson disease. *Molecular and cellular biochemistry* **418**(1-2)**:** 59-70.

Osei-Hyiaman D, DePetrillo M, Pacher P, Liu J, Radaeva S, Batkai S*, et al.* (2005). Endocannabinoid activation at hepatic CB1 receptors stimulates fatty acid synthesis and contributes to diet-induced obesity. *The Journal of clinical investigation* **115**(5)**:** 1298-1305.

Pacher P, Mechoulam R (2011). Is lipid signaling through cannabinoid 2 receptors part of a protective system? *Progress in lipid research* **50**(2)**:** 193-211.

Rajesh M, Mukhopadhyay P, Hasko G, Huffman JW, Mackie K, Pacher P (2008). CB2 cannabinoid receptor agonists attenuate TNF-alpha-induced human vascular smooth muscle cell proliferation and migration. *British journal of pharmacology* **153**(2)**:** 347-357.

Rehg JE, Bush D, Ward JM (2012). The utility of immunohistochemistry for the identification of hematopoietic and lymphoid cells in normal tissues and interpretation of proliferative and inflammatory lesions of mice and rats. *Toxicologic pathology* **40**(2)**:** 345-374.

Shepard BD, Tuma PL (2009). Alcohol-induced protein hyperacetylation: mechanisms and consequences. *World journal of gastroenterology* **15**(10)**:** 1219-1230.

Silvestri C, Di Marzo V (2013). The endocannabinoid system in energy homeostasis and the etiopathology of metabolic disorders. *Cell metabolism* **17**(4)**:** 475-490.

Stienstra R, Saudale F, Duval C, Keshtkar S, Groener JE, van Rooijen N*, et al.* (2010). Kupffer cells promote hepatic steatosis via interleukin-1beta-dependent suppression of peroxisome proliferator-activated receptor alpha activity. *Hepatology* **51**(2)**:** 511-522.

Tam J, Cinar R, Liu J, Godlewski G, Wesley D, Jourdan T*, et al.* (2012). Peripheral cannabinoid-1 receptor inverse agonism reduces obesity by reversing leptin resistance. *Cell metabolism* **16**(2)**:** 167-179.

Tam J, Liu J, Mukhopadhyay B, Cinar R, Godlewski G, Kunos G (2011). Endocannabinoids in liver disease. *Hepatology* **53**(1)**:** 346-355.

Teixeira-Clerc F, Belot MP, Manin S, Deveaux V, Cadoudal T, Chobert MN*, et al.* (2010). Beneficial paracrine effects of cannabinoid receptor 2 on liver injury and regeneration. *Hepatology* **52**(3)**:** 1046-1059.

Teixeira-Clerc F, Julien B, Grenard P, Tran Van Nhieu J, Deveaux V, Li L*, et al.* (2006). CB1 cannabinoid receptor antagonism: a new strategy for the treatment of liver fibrosis. *Nature medicine* **12**(6)**:** 671-676.

This article is protected by copyright. All rights reserved.

Tsai WW, Matsumura S, Liu W, Phillips NG, Sonntag T, Hao E*, et al.* (2015). ATF3 mediates inhibitory effects of ethanol on hepatic gluconeogenesis. *Proceedings of the National Academy of Sciences of the United States of America* **112**(9)**:** 2699-2704.

Tsung A, Hoffman RA, Izuishi K, Critchlow ND, Nakao A, Chan MH*, et al.* (2005). Hepatic ischemia/reperfusion injury involves functional TLR4 signaling in nonparenchymal cells. *Journal of immunology* **175**(11)**:** 7661-7668.

Wang M, You Q, Lor K, Chen F, Gao B, Ju C (2014). Chronic alcohol ingestion modulates hepatic macrophage populations and functions in mice. *Journal of leukocyte biology* **96**(4)**:** 657-665.

Wu C, Jia Y, Lee JH, Jun HJ, Lee HS, Hwang KY*, et al.* (2014). trans-Caryophyllene is a natural agonistic ligand for peroxisome proliferator-activated receptor-alpha. *Bioorganic & medicinal chemistry letters* **24**(14)**:** 3168-3174.

Yin H, Hu M, Liang X, Ajmo JM, Li X, Bataller R*, et al.* (2014). Deletion of SIRT1 from hepatocytes in mice disrupts lipin-1 signaling and aggravates alcoholic fatty liver. *Gastroenterology* **146**(3)**:** 801-811.

Zheng X, Sun T, Wang X (2013). Activation of type 2 cannabinoid receptors (CB2R) promotes fatty acid oxidation through the SIRT1/PGC-1alpha pathway. *Biochemical and biophysical research communications* **436**(3)**:** 377-381.

Accepted Article

This article is protected by copyright. All rights reserved.

Figure Legends

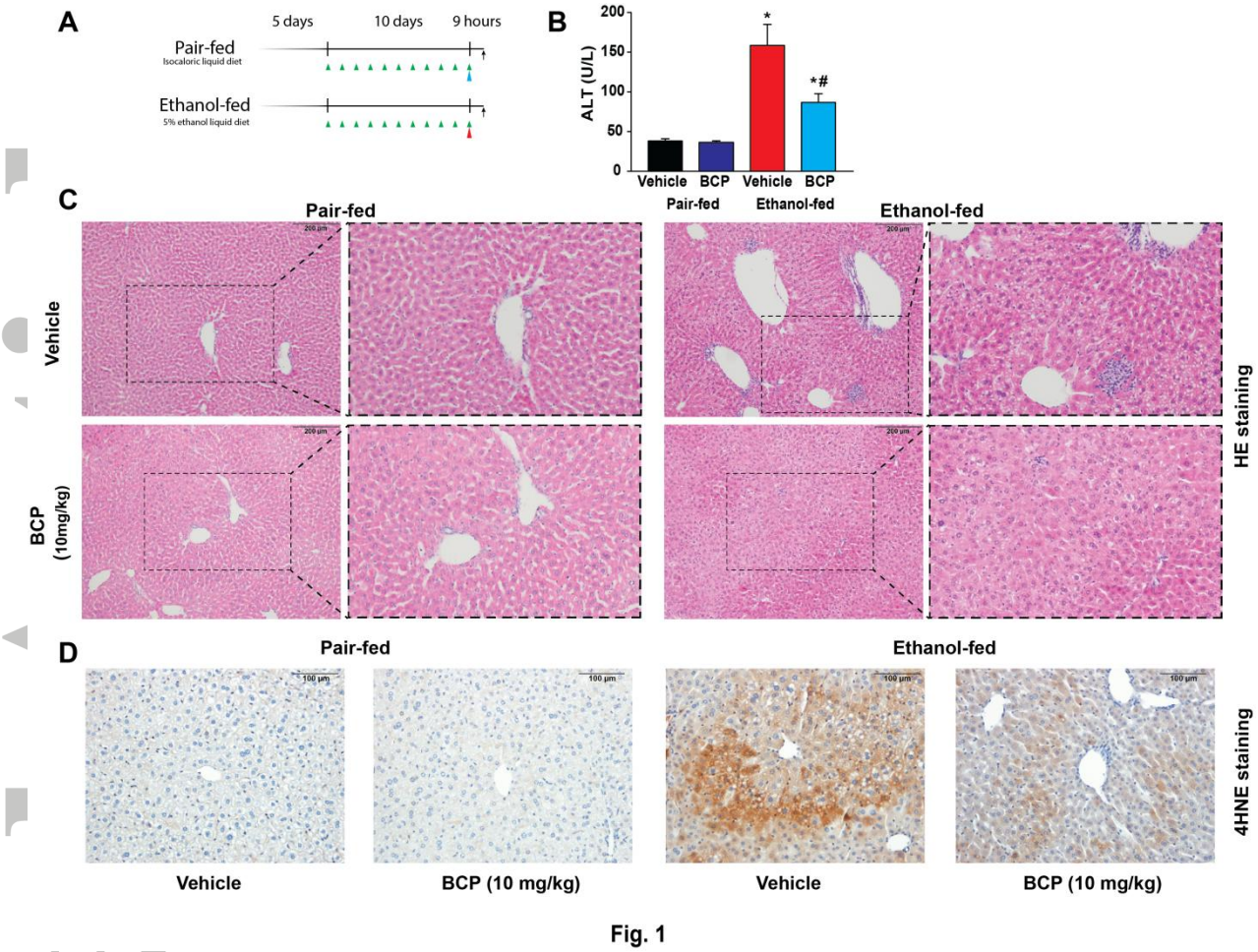

Fig. 1

Fig. 1. Protective effect of β-caryophyllene treatment against chronic plus binge ethanol feeding induced hepatic injury

(**A**) Experimental alcohol- and isocaloric pair-feeding protocol combined with single ethanol/maltodextrin binge at the end of the 10 days long diet. Green arrows indicate daily drug treatments (vehicle or 10 mg/kg BCP). Red arrow represents single ethanol binge treatment, while the blue arrow represents an isocaloric maltodextrin gavage.

(**B**) Determination of liver injury by measurement of ALT enzyme activity, and histological assessment of hepatic pathologic alterations (**C**) on hematoxylin-eosin stained liver sections in vehicle or BCP treated pair-fed or ethanol-fed mice, respectively.

(**D**) Assessment of oxidative stress in vehicle or BCP treated pair-fed or ethanol-fed mice, by histological staining for 4-hydroxy-nonenal.

Results are mean ± S.E.M. n= 8. *p<0.05 vs. pair-fed with vehicle treatment, #p<0.05 vs. ethanol-fed with vehicle pretreatment.

This article is protected by copyright. All rights reserved.

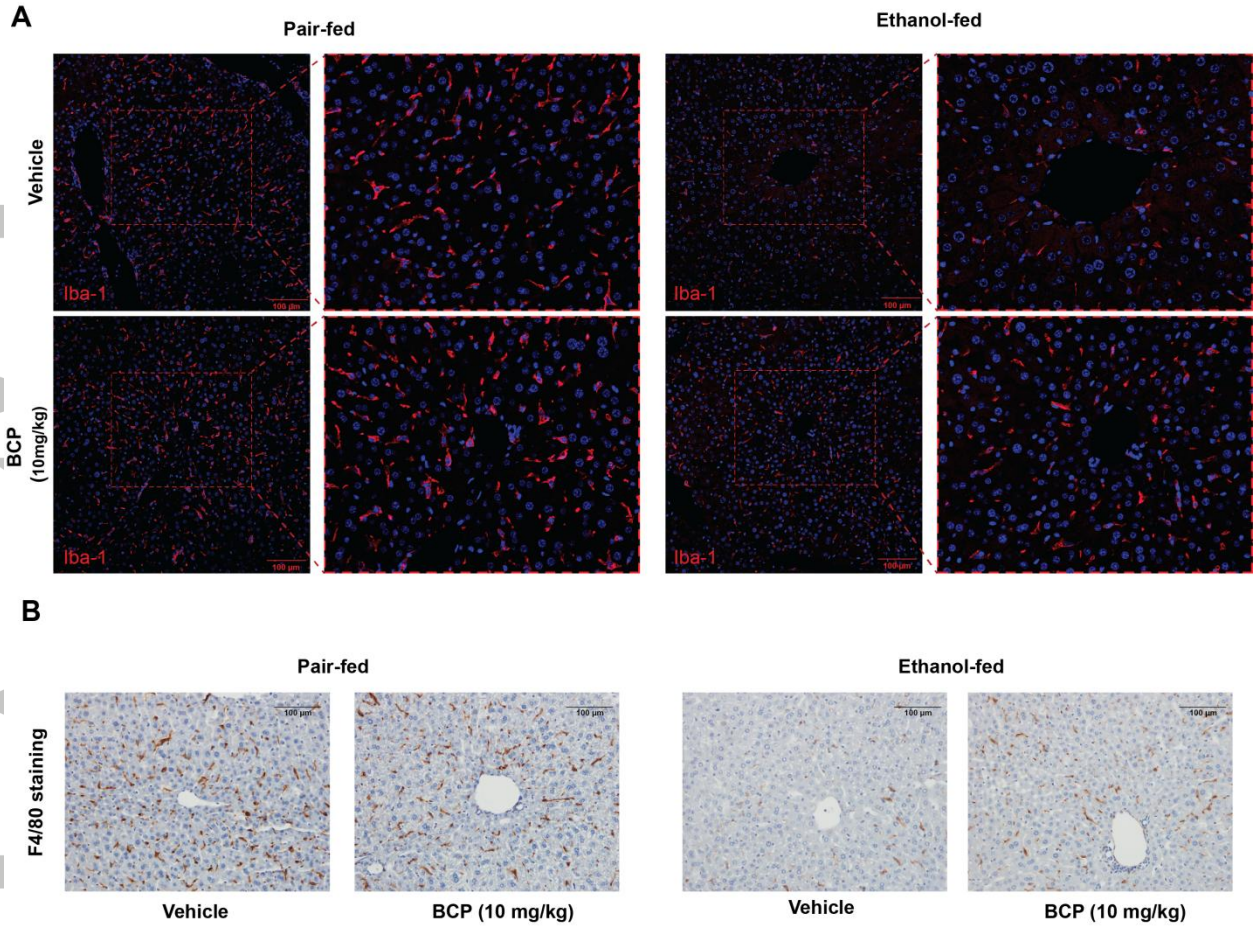

Fig. 2

Fig. 2. β-caryophyllene prevents chronic plus binge ethanol feeding-induced morphological changes in hepatic macrophages

(A) Representative confocal scanning microscopic images of Iba-1 positive hepatic macrophages from pair-fed and ethanol-fed mice either treated with vehicle or BCP (10 mg/kg). (**B**) Representative light microscopic images of F4/80 positive hepatic macrophages from pair-fed and ethanol-fed mice either treated with vehicle or BCP (10 mg/kg).

Accepted

This article is protected by copyright. All rights reserved.

Accepted Article

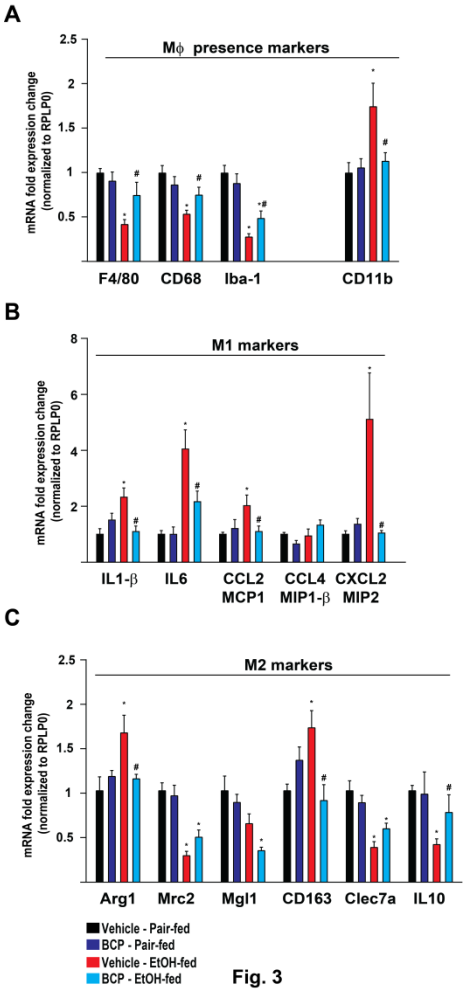

Fig. 3. β-caryophyllene prevents chronic plus binge ethanol feeding-induced pro-inflammatory phenotypic switch of hepatic macrophages

(A) Gene expression of classic macrophage markers, F4/80, CD68, Iba-1, and CD11b in the liver of pair-fed and ethanol-fed mice either treated with vehicle or BCP (10 mg/kg). (**B**) Gene expression of pro-inflammatory macrophage activation markers (M1 phenotype), IL-1-β, IL-6, CCL2, CCL4, and CXCL2 in the liver of pair-fed and ethanol-fed mice either treated with vehicle or BCP (10 mg/kg). (**C**) Gene expression of alternative macrophage activation markers (M2 phenotype), Arg-1, Mrc-2, Mgl-1, CD163, Clec7a, and IL-10 in the liver of pair-fed and ethanol-fed mice either treated with vehicle or BCP (10 mg/kg).

Results are mean ± S.E.M. n= 6. *p<0.05 vs. pair-fed with vehicle treatment, #p<0.05 vs. ethanol-fed with vehicle pretreatment.

This article is protected by copyright. All rights reserved.

Accepted Article

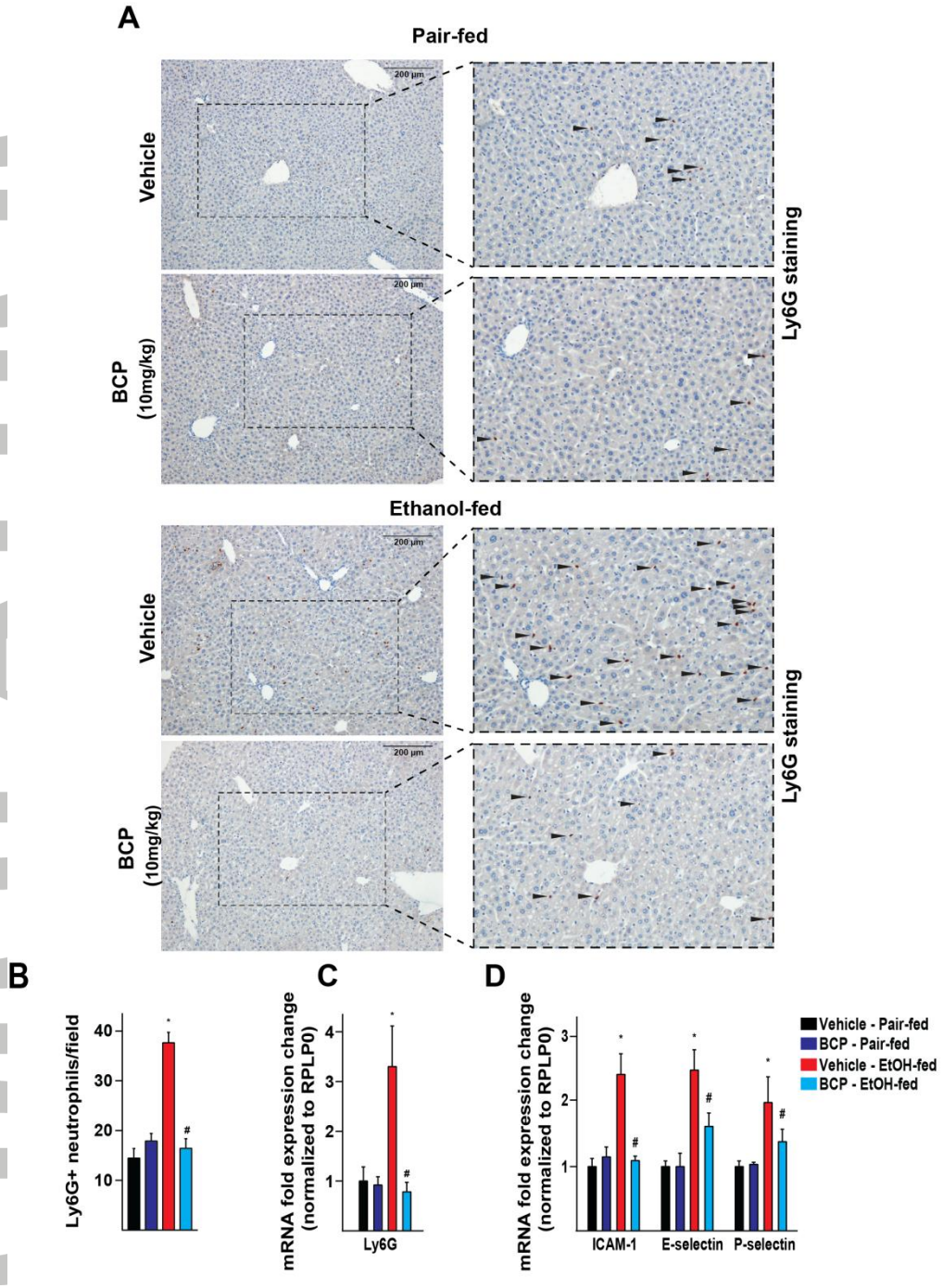

Fig. 4

Fig. 4. β-caryophyllene prevents chronic plus binge ethanol feeding-induced hepatic vascular inflammation and neutrophil infiltration

(**A**) Immunohistochemical detection of Ly6G positive neutrophil granulocytes from pair-fed and ethanol-fed mice either treated with vehicle or BCP (10 mg/kg). (**B**) Average number of neutrophil granulocytes on high power field microscopic images taken from histological sections of the livers of pair-fed and ethanol-fed mice either treated with vehicle or BCP (10 mg/kg). (**C**) Gene expression of the neutrophil marker Ly6G in the liver of pair-fed and

This article is protected by copyright. All rights reserved.

ethanol-fed mice either treated with vehicle or BCP (10 mg/kg). (**D**) Gene expression of pro-inflammatory vascular adhesion molecules, ICAM-1, E-selectin, and P-selectin in the liver of pair-fed and ethanol-fed mice either treated with vehicle or BCP (10 mg/kg).
Results are mean ± S.E.M. n= 6. *$p<0.05$ vs. pair-fed with vehicle treatment, #$p<0.05$ vs. ethanol-fed with vehicle pretreatment.

Accepted Article

This article is protected by copyright. All rights reserved.

Accepted Article

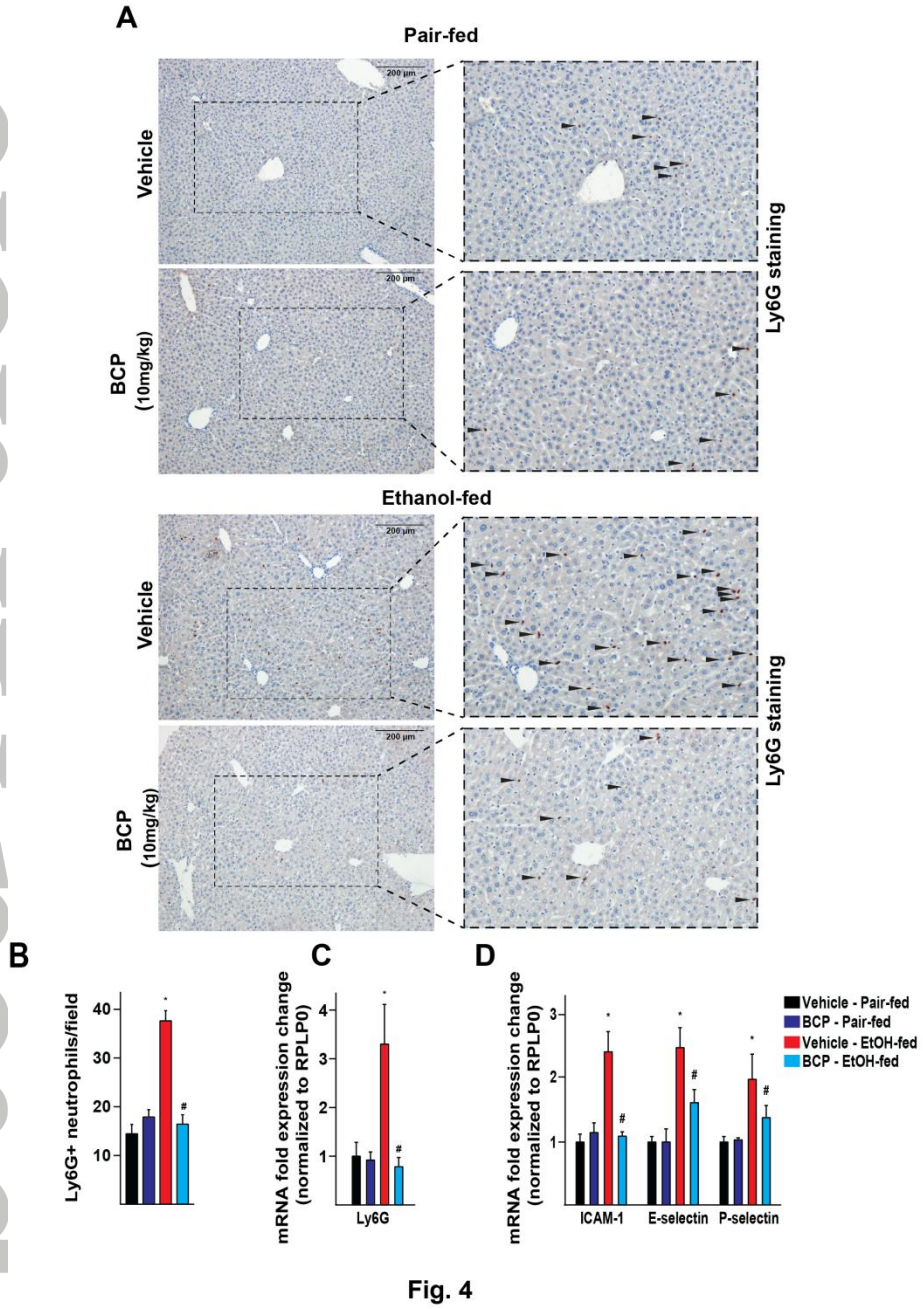

Fig. 4

Fig. 5. β-caryophyllene prevents chronic plus binge ethanol feeding-induced hepatic steatosis

(**A**) Histochemical detection of neutral lipids (Oil Red O staining) in fresh frozen liver sections of pair-fed and ethanol-fed mice either treated with vehicle or BCP (10 mg/kg). (**B**) Quantitative determination of triglycerol content in the livers of pair-fed and ethanol-fed mice either treated with vehicle or BCP (10 mg/kg).

Results are mean ± S.E.M. n= 6.*p<0.05 vs. pair-fed with vehicle treatment, #p<0.05 vs. ethanol-fed with vehicle pretreatment.

This article is protected by copyright. All rights reserved.

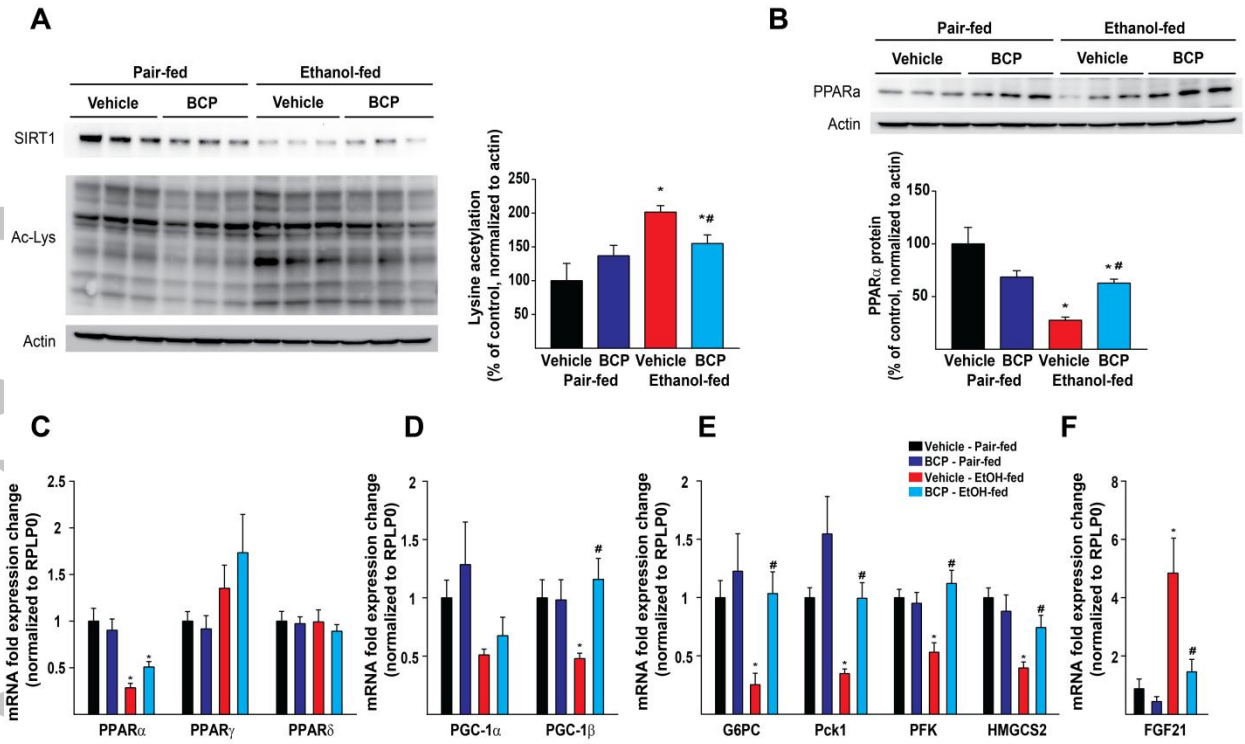

Fig. 6

Fig. 6. β-caryophyllene prevents chronic plus binge ethanol feeding-induced loss of PPARα expression, decreases protein hyperacetylation and promotes PPARα-dependent signaling

Western blot analysis of hepatic protein lysine acetylation (**A and B**) and PPARα protein expression (**B**) in the liver of pair-fed and ethanol-fed mice either treated with vehicle or BCP (10 mg/kg). (**C**) Gene expression of PPAR transcription factors, PPARα, PPARγ, and PPARδ in the liver of pair-fed and ethanol-fed mice either treated with vehicle or BCP (10 mg/kg). (**D**) Gene expression of PPAR coactivators, PGC1-α, and PGC1-β in the liver of pair-fed and ethanol-fed mice either treated with vehicle or BCP (10 mg/kg). (**E**) Gene expression of PPARα signaling-related transcripts, G6PC, PCK-1, PFK, HMGCS2 and (**F**) FGF-21 in the liver of pair-fed and ethanol-fed mice either treated with vehicle or BCP (10 mg/kg).

Results are mean ± S.E.M. n= 6. *p<0.05 vs. pair-fed with vehicle treatment, #p<0.05 vs. ethanol-fed with vehicle pretreatment.

This article is protected by copyright. All rights reserved.

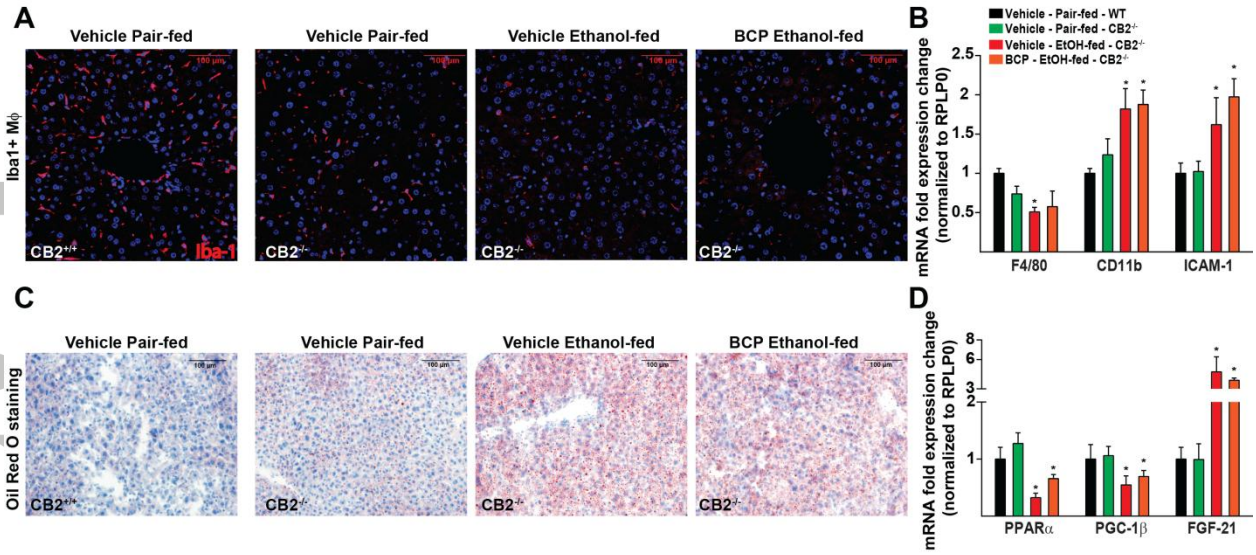

Fig. 7

Fig. 7. β-caryophyllene-induced protection against alcoholic steatohepatitis is attenuated in CB2 receptor deficient mice

(**A**) Confocal scanning microscopic images of Iba-1 positive hepatic macrophages from pair-fed wild type CB2 receptor deficient mice and from ethanol-fed CB2 receptor deficient mice either treated with vehicle or BCP (10 mg/kg). (**B**) Gene expression of classic macrophage markers, F4/80, and the pro-inflammatory vascular adhesion molecule ICAM-1 and the monocyte marker CD11b in the liver of pair-fed and ethanol-fed CB2 receptor deficient mice either treated with vehicle or BCP (10 mg/kg). (**C**) Histochemical detection of neutral lipids (Oil Red O staining) in fresh frozen liver sections of pair-fed wild type CB2 receptor deficient mice and from ethanol-fed CB2 receptor deficient mice either treated with vehicle or BCP (10 mg/kg). (**D**) Gene expression of PPARα, PGC1-β and FGF21 in the liver of pair-fed and ethanol-fed CB2 receptor deficient mice either treated with vehicle or BCP (10 mg/kg).

Results are mean ± S.E.M. n= 6. *p<0.05 vs. sham with vehicle pretreatment.

This article is protected by copyright. All rights reserved.

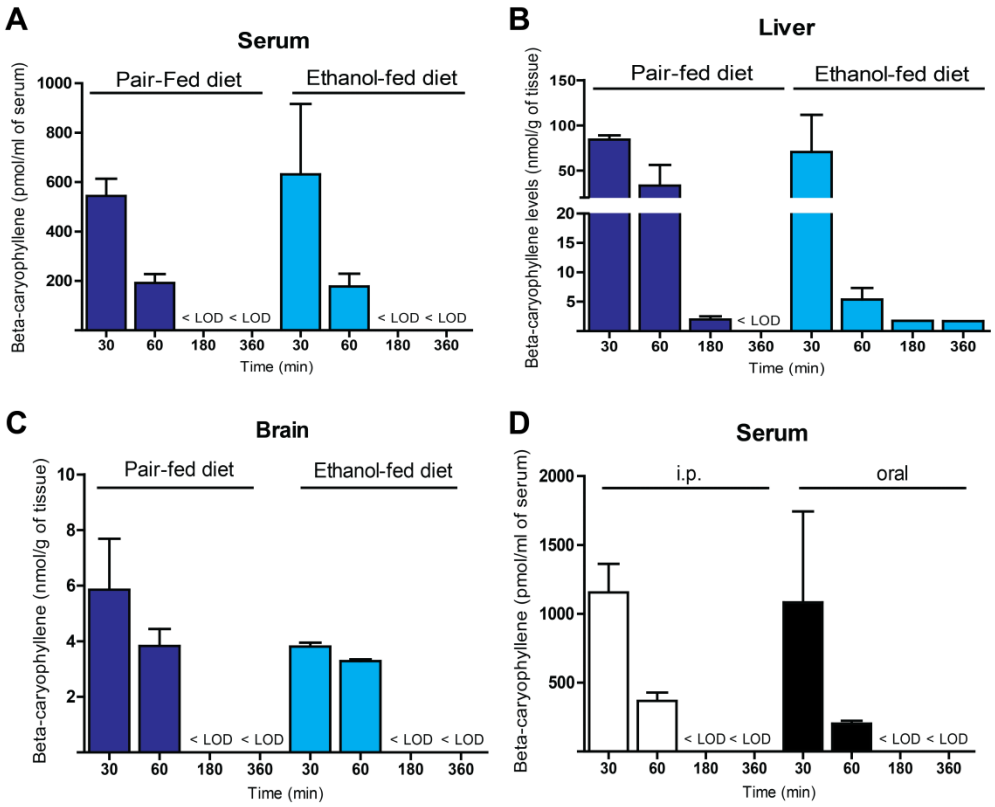

Fig. 8. Pharmacokinetic properties of β-caryophyllene

(**A**) Determination of serum, hepatic (**B**), and brain (**C**) tissue levels of BCP 30, 60, 180, and 360 min after 10 day long chronic administration (10 mg/kg daily) to either pair-fed or ethanol-fed animals. (**D**) Determination of serum levels of BCP 30, 60, 180, and 360 min after BCP administration (single dose of 10 mg/kg given intraperitoneally [i.p.] or orally). Results are mean ± S.E.M. n= 3.

Accepted

This article is protected by copyright. All rights reserved.